HEFAT2012
9th International Conference on Heat Transfer, Fluid Mechanics and Thermodynamics
16 – 18 July 2012
Malta

SIMULTANEOUS HEAT AND MASS TRANSFER INSIDE A HEATED CAVITY WITH A MOISTURE SOURCE

Kayihan A.S.* and Onbasioglu S.**
*Author for correspondence
Arcelik AS, R&D Department
Tuzla, Istanbul, 34950
TURKEY,
E-mail: asli.kayihan@arcelik.com

**Istanbul Technical University
Gumussuyu, Istanbul, 34473
TURKEY

ABSTRACT

In many engineering problems, momentum, energy and mass transport take place together and these equations must be analyzed simultaneously. Especially in food industry, the most important step of processes like cooking, drying, smoking is the simultaneous heat and mass transfer. During these processes, significant changes in physical, chemical and nutritional properties of food occur. Most of these changes are functions of temperature, humidity and time.

In cavities with moisture sources, investigating simultaneous heat and mass transfer is important to reveal the behavior of the system. In this study, an experimental and numerical investigation was carried out on the simultaneous heat and mass transfer inside a heated cavity which has a moisture source in it. For analyzing simultaneous heat and mass transfer, a model of a heated cavity having a porous mass source (brick) was established. For analysis studies, commercial FLUENT® software which solves basic momentum, energy and mass transport equations is used. In order to express the vaporization of the water in the brick, an external code is written. Within the scope of experimental studies, a cavity which had a water soaked brick within was used. The brick was heated by hot air which was forwarded into cavity. During the tests, the temperature change in the cavity and brick were recorded. In order to express the mass loss of the brick, the mass change of the brick was also recorded. The boundary values which are needed in the modeling studies were determined experimentally. The results of the analysis studies implemented were compared with the experimental results and good agreement was observed for the temperature of the brick and the mass loss of the brick.

INTRODUCTION

For modeling of the simultaneous heat and mass transfer, the computational domain generally includes the load, through which the water is vaporized. However, in most of the studies reported in literature, the cavity air in which the load stands is not involved. Indeed, as the load is heated up, its water content evaporates and diffuses into the cavity air. Instead of modeling the surrounding cavity air, the interaction between the load and the cavity air is usually constructed through the boundary conditions [1-4]. Thorvaldsson &Janestad [2] solve also the one dimensional diffusion of liquid water However, other studies deal only with the vapour diffusion, Neale et al. [5] for example implement an external MATLAB code to FLUENT® to solve the vapor transport within the load.

NOMENCLATURE

A	[m^2]	Total heat transfer area
C	[kg water/kg dry air]	Water vapor concentration
C_2	[m^{-1}]	Inertial resistance term
C_p	[J/kgK]	Specific Heat
$cpgc$	[kg/(m^3sPa)]	Combined pressure gradient coefficient
D_{AB}	[m^2/s]	Diffusion coefficient
g	[m/s^2]	Gravitational acceleration
h	[W/(m^2K)]	Convection heat transfer coefficient
h_{fg}	[J/kg]	Enthalpy of vaporization
h_m	[m/s]	Convection mass transfer coefficient
L	[m]	Characteristic length
m_{wv}	[kg]	Mass of water vaporized
P	[Pa]	Pressure
P_{sat}	[Pa]	Partial pressure of the air on the faces of the voids in the solid part of the brick
P_{satinf}	[Pa]	Saturation pressure of the water vapor in brick voids
q	[J]	Energy of vaporization
$\dot{Q}$	[W]	Heat
S	[-]	Source term
spv	[m^2/m^3]	Surface per volume
t	[s]	Time
T	[°C, K]	Mean temperature

U	[m/s]	Velocity
UDF	[-]	User defined function
u_i	[m/s]	Mean velocity
u_i'	[m/s]	Velocity fluctuation

Greek Symbols

α	[m^2]	Permeability
β	[-]	Relaxation factor
ΔP	[Pa]	Vapor pressure difference
Δy	[m]	Layer thickness
ϕ	[W/m^3]	Turbulent dissipation
Γ	[kg/(msPa)]	Water vapor permeability
μ	[kg/ms]	Dynamic viscosity
ν	[m^2/s]	Kinematic viscosity
ρ	[kg/m^3]	Density

Subscripts

∞	Free stream
amb	Ambient
n	Normal
s	Surface
wv	Water vapor

Some of modeling approaches are supported by experimental data which help to express diffusion mechanisms [3, 6].

There are a few studies solving the governing equations for both the load and the cavity air via external codes added to FLUENT® solvers. Le Page et al. [7] used "User Defined Functions (UDFs)" to express the relationship between the load and the cavity air. However, the computational domain for the air flow is limited with a small user defined volume surrounding the food. Besides, in many of real applications, the load has a porous structure which should be taken into account.

To make a more realistic approach, in the current research, simultaneous heat and mass transfer between the cavity and the porous brick has been modeled, considering the porous brick as the source of the humidity releasing water vapour into the cavity. Special care has been given to the porous structure of the brick and the mass transfer through the boundaries separating the brick and the cavity zones.

EXPERIMENTAL SET-UP

To validate the model, a cavity having dimensions 230 mmx230 mmx130 mm was designed. The brick was water soaked and inserted within the cavity where it was heated by hot air stream (Figure 1). During the tests, the temperature change in the cavity and both the temperature and mass changes of the brick were recorded. The variables for the external boundaries and the initial values such as air inlet velocity and cavity temperature were also measured to use in the computational modeling.

In the experimental setup (Figure 1), the cavity was surrounded by an insulation layer of 20 mm thickness. In the upper face of this cavity, there is an opening with square cross section (20 mmx20 mm) ventilation. The cavity is connected to a channel with an axial fan installed at the inlet section, to simulate the forced convection conditions. The mean velocity measured at the entrance of the channel by hot wire anemometer is 3m/s.

The heater in the channel section, close to the cavity, heats the air blown by the fan. In order to maintain temperature in the cavity at 70°C, 360 W power has been applied to the heater.

The experimental setup was placed on a scale to measure the mass loss of the brick specified in the energy consumption standard [8]. Only one fourth portion of this standard brick was used.

After the temperature of the cavity reached to the desired value, the water soaked brick at 5°C was placed in the center of the cavity. The heated air, directly forwarded into the cavity passed over the brick and left from the opening, so called chimney in Figure 1. During the experiments, the temperature of the brick center was measured by J type thermocouples.

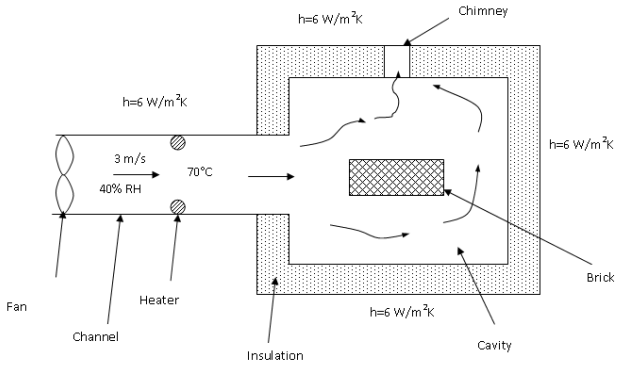

Figure 1 The experimental setup and estimated flow pattern of the hot air stream through the cavity

COMPUTATIONAL MODEL

The modeling process is based on the balance between i) the production rate of water vapor within the brick, ii) the rate of vapor transfer from the brick surfaces to the cavity, and iii) the rate of vapor transfer in the cavity through the opening.

In FLUENT®, the following transport equations below are solved:

Continuity:

$$\frac{\partial \rho}{\partial t} + \frac{\partial (\rho u_i)}{\partial x_i} = 0 \qquad (1)$$

Momentum:

$$\rho \frac{Du_i}{Dt} = \frac{\partial p}{\partial x_i} + \frac{\partial}{\partial x_j}\left[\mu\left(\frac{\partial u_i}{\partial x_j} + \frac{\partial u_j}{\partial x_i}\right) - \rho\overline{u_i' u_j'}\right] + \rho g_i \qquad (2)$$

where $-\rho\overline{u_i' u_j'}$ is the turbulent shear stress.

Energy:

$$\rho C_p \frac{DT}{Dt} = k\frac{\partial^2 T}{\partial x_i^2} + \mu\frac{\partial u_i}{\partial x_j}\left(\frac{\partial u_i}{\partial x_j} + \frac{\partial u_j}{\partial x_i}\right) + \frac{\partial}{\partial x_i}\left(-C_p\rho\overline{u_i' T'}\right) + \phi' + S_{ener} \qquad (3)$$

Mass:

$$\rho \frac{DC}{Dt} = \frac{\partial}{\partial x_i}\left(D_{AB} \frac{\partial(\rho C)}{\partial x_i} - \rho \overline{u_i' C'} \right) + S_{mass} \quad (4)$$

Water vapor transport was possible to be involved in the computations just by activating the "species" model [9]. However, the source terms, the last terms in equations (3) and (4), are not contributed to the computations without implementing an external code. S_{mass}, which will be denoted as m_{wv}''' represents the vapor generation, and the heat destruction due to this vaporization, S_{ener}, is equal to vapor generation times the latent heat. In the current study, these source terms have been added to the mass transport and energy equations using UDFs.

The Reynolds number for the flow in the cavity was calculated as

$$\mathrm{Re} = \frac{UL}{\nu} \approx 45{,}000 \quad (5)$$

based on the length of the cavity, 0.23 m, and the velocity measured at the inlet of the channel (Figure 1), 3 m/s. Reynolds number value calculated in Eq. (5) corresponds to turbulence in an enclosure where forced convection dominates.

Various Reynolds Avarage Navier Stokes (RANS) models had been applied to compute the turbulent flow. Realizable k-ε model having the advantages of lower computational time and satisfactory compliance with the experimental results was chosen [10].

Since the convection outside the cavity is natural, the order of magnitude for h, is O (10). Velocity and temperature values, 3 m/s and 70°C (Figure 1) at the channel inlet were implemented from experimental results. For the turbulence parameters at the inlet, the hydraulic diameter was calculated using channel cross section dimensions 100 mmx100 mm. The specific humidity value of the air entering the channel was taken constant, corresponding to 40% relative humidity at ambient temperature, which is 10 g water/kg dryair.

When determining the boundary conditions for the brick, the porous structure was taken into account. This consideration is possible by means of a source term added to the momentum equation (Eq. (2));

$$S_i = -\left(\mu \frac{1}{\alpha} U_i - + C_2 \frac{1}{2} \rho U_i^{\,2} \right) \quad (6)$$

where α is permeability and C_2 is inertial resistance factor. 1/ α corresponds to viscous losses.

When a mass generator exists, modeling the mass transfer through the boundaries is challenging in FLUENT®. In the current study, boundary types such as i-) interior, ii-) wall and iii-) porous jump were tested and "interior" boundary condition was chosen.

In case of "wall" type boundary condition being applied on the brick surfaces, either the "species" variable should be specified or the mass flux should be equalized to zero. However, both of these conditions are unrealistic for the current problem. To determine the real value of the specified mass flux on the brick surfaces, the following equation was implemented through a UDF.

$$h_m (C_s - C_\infty) = -D_{AB} \left(\frac{\partial C}{\partial x_n} \right)_{boundary} \quad (7)$$

resulting in

$$C_S = \frac{1}{h_m} \left(C_\infty - D_{AB} \frac{\partial C}{\partial x}\bigg|_{boundary} \right) \quad (8)$$

In the above equations D_{AB} is the diffusivity, C is the water vapor content and h_m is the convective mass transfer coefficient. Calculating the species on the brick surfaces, C_S, with Eq. (8) means to apply Drichlet boundary condition which results in uncoupled water vapor fields in the brick and the cavity (Figure 2).

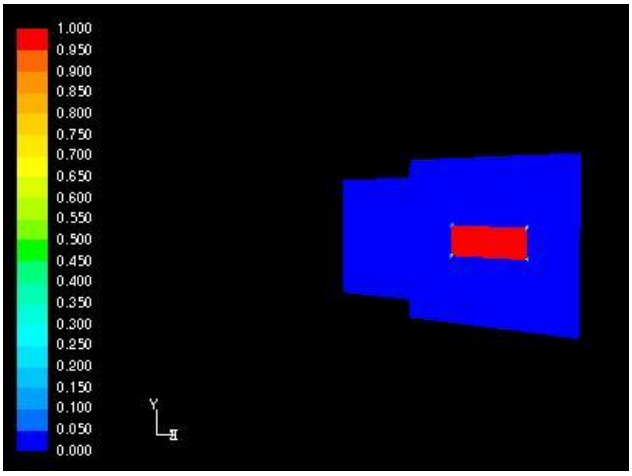

Figure 2 Mass fraction distribution of water vapor with "wall" type boundary conditions on the brick surfaces

As seen in Figure 2, when wall type boundary condition was applied, the interaction between the brick and the cavity could not be established and consequently, mass transfer between the brick and the cavity did not occur. Le Page et al. [7] also refer to this boundary type problem. Unfortunately, coupled or Drichlet type boundary condition does not exist in FLUENT® for species transport.

To reach to an interactive transfer of the vapor between the two zones, namely, the brick and the cavity, "porous jump" type boundary condition was also applied. However, it just forms an extended porous volume around the brick. Thus, the "interior" type boundary condition, allowing the mass interaction between the porous brick and the cavity was applied to the brick surfaces.

MASS TRANSFER MODEL AND USER DEFINED FUNCTIONS

The air in the voids of the water soaked brick is assumed as saturated (100% relative humidity).

For the porous brick, the momentum equation (Eq. (2)) with the source term given in Eq. (6) is solved. Adding to that, due to the local specific humidity differences within the solid and void parts of the brick, the transport equation for the species (Eq. (4)) is solved.

As the brick is heated up, the water in the solid parts evaporates and passes to the voids of the brick (Figure 3) but Eq. (4) is not sufficient to represent the evaporation through the solid parts into the brick voids.

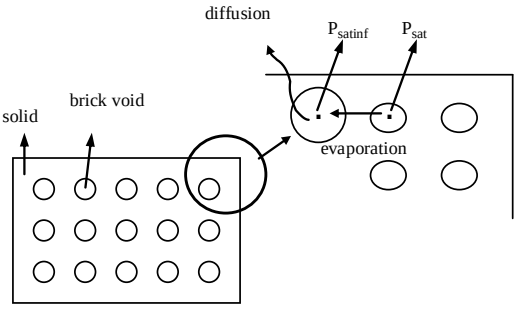

Figure 3 Evaporation and diffusion in the brick

To express the vaporization of the water in the solid parts of the brick, simple "dew point" method for drying in porous structures given in [10] was used. Mass flux on water soaked surfaces of the brick to air is calculated by this method as the following:

$$\dot{m}''_{wv} = -\Gamma \frac{\Delta P}{\Delta y} \tag{9}$$

where m_{wv}'' is the water vapor flux through a layer of material, Γ is the water vapor permeability of the material (mass penetrated through a unit area per unit time); ΔP is the vapor pressure difference across the layer. Δy is the thickness of the layer. To be able to express the amount of water vaporized in the brick volume, Eq. (9) is multiplied by "surface per unit volume (spv)" factor and substituted in Eq. (4):

$$\dot{m}'''_{wv} = -\Gamma.spv.\frac{\Delta P}{\Delta y} \tag{10}$$

With an approach which takes the brick as a bulk structure, instead of boundary layer thickness, the Δy value was taken as the characteristic length of the brick. Using these three constants; the combined pressure gradient coefficient "cpgc" preceding the pressure difference in Eq. (10) is formed as

$$cpgc = \frac{\Gamma.spv}{\Delta y} \tag{11}$$

and implemented through the UDF code and amount of water vaporized per unit time and unit volume is calculated:

$$\dot{m}'''_{wv} = -cpgc.\left(P_{sat} - P_{sat\,\inf}\right) \tag{12}$$

Here, P_{sat} and P_{satinf} are the partial pressure values of the vapor, on the faces of the voids and within the voids, respectively.

Using the appropriate values for the brick used in the experiments, the vapor generation through the water soaked brick was computed and the vaporization heat was added to the basic energy equation (Eq. (3)) as a source term with a computational relaxation factor, β:

$$\dot{q}''' = \beta \dot{m}'''_{wv} h_{fg} \tag{13}$$

The flow chart composed to solve the simultaneous heat and mass transfer is given in Figure 4. The i, ii and vi steps are solved by FLUENT® main solvers. In step iii, the equations (12) and (13) are solved based on the steps iv and v where the relations between UDFs and FLUENT® main solver are established. To add the source terms to FLUENT® software, the codes were written in C++.

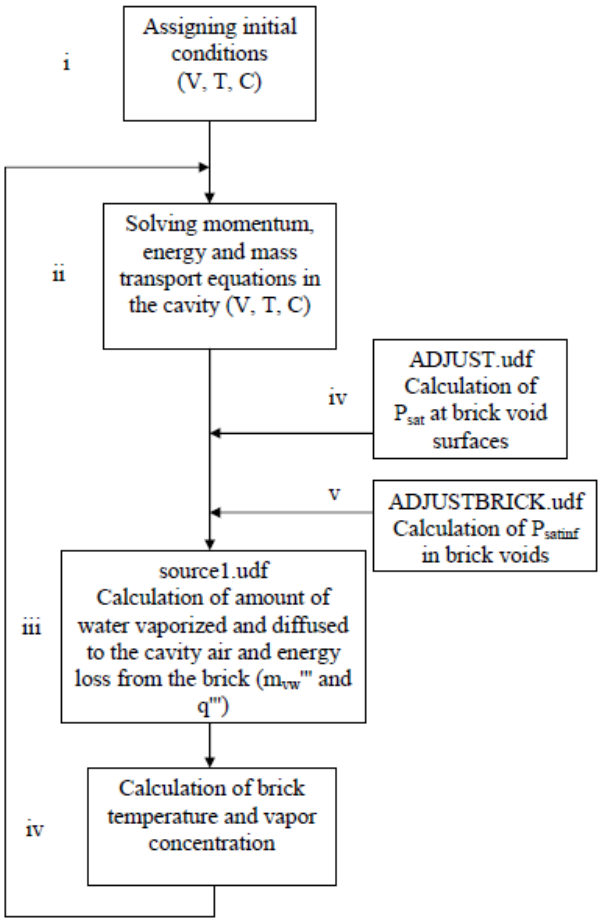

Figure 4 Simultaneous heat and mass transfer solution flow chart

By the method explained here, simultaneous heat and mass transport equations were solved for both water soaked brick and

the interacting cavity, excluding the liquid water. Such an attempt, namely solving a cavity problem with a humidity source, including the liquid water transport equation is present in literature [6]. Such an approach needs a long computational time; even it is 1D simulation. The same problem has been solved with the methodology presented in our current study for the validation purposes [12].

RESULTS AND DISCUSSION

The temperature distribution in the brick center plane obtained from the computational studies (at t=6000 seconds) with the constants given above is illustrated in Figure 5.

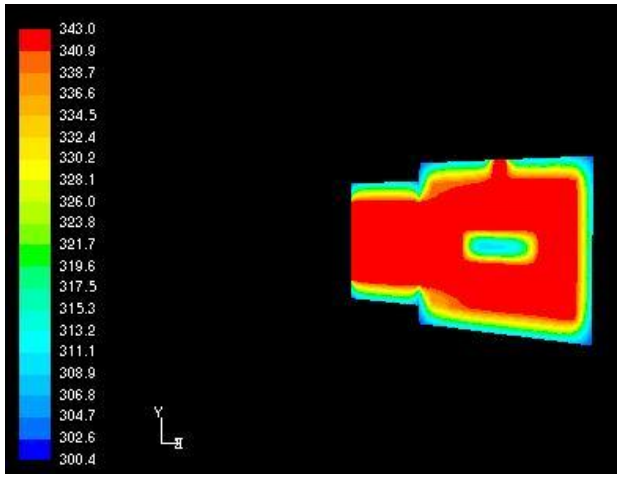

Figure 5 Temperature distribution [K] in the center plane of the brick

As can be seen from the figure, the temperature of the cavity has reached the inlet condition of 343 K. The coldest region is the brick center and the lowest brick temperature is 307 K.

Water vapor concentration distribution in the center plane of the brick is given in Figure 6.

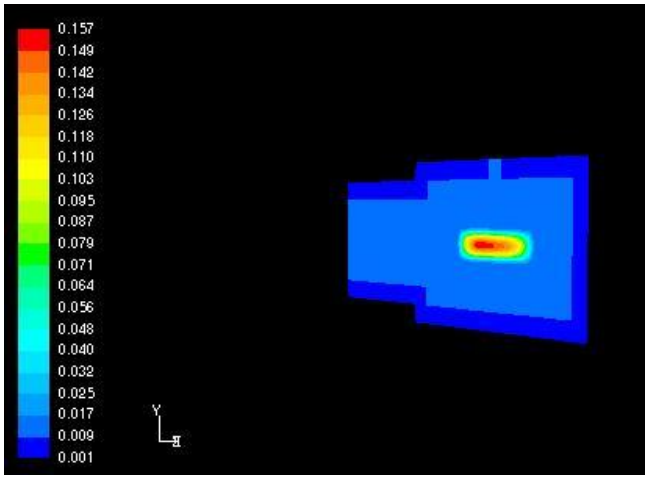

Figure 6 Mass fraction distribution of water vapor in the center plane of the brick

The highest water vapor concentration occurs at the center of the brick. The water vapor concentrations in the regions near the brick surfaces decrease as a result of diffusion and vaporization, implying that brick dries.

The temperature change of the brick center gained by both experiments and computational studies is given in Figure 7.

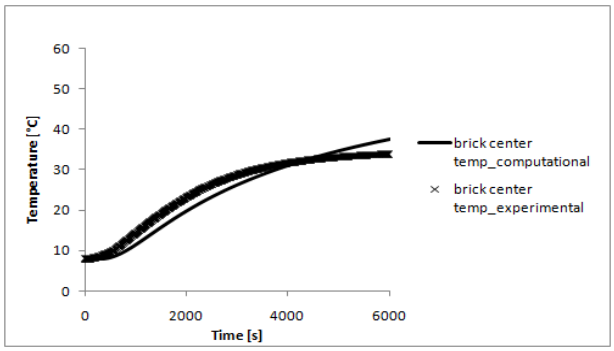

Figure 7 Compared brick center temperature

As can be seen from the figure, the maximum brick center temperature difference between the experiments and computations is 3.5 K.

The overall flow modeling (turbulence models) may cause the difference between the computational and experimental results. However as indicated above, various Reynolds Avarage Navier Stokes (RANS) models had been applied to compute the turbulent flow and there is not a significant difference between the Reynolds Avarage Navier Stokes (RANS) models (Figure 8).

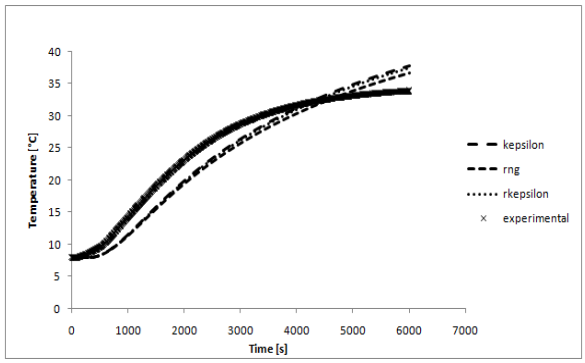

Figure 8 Brick center temperature with different turbulence models

The mass loss of the brick gained by both experiments and computational studies is given in Figure 9.

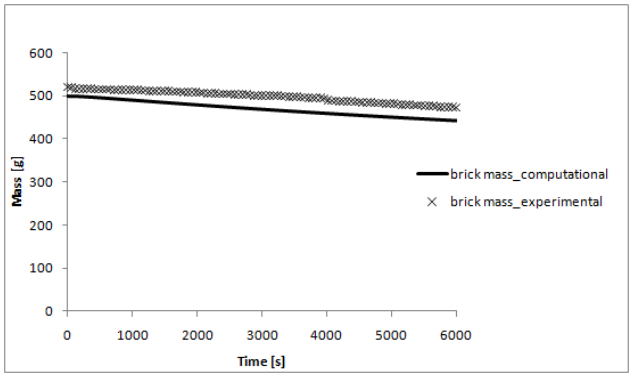

Figure 9 Compared brick mass loss

The mass loss of the brick gained from the computational studies is slightly lower than the experimental results. This situation is expected since the temperature gained by the computational studies is higher than the experimental ones (Figure 7).

When the results of the computational studies for the model implemented to solve the simultaneous heat and mass transfer are compared with the experimental results, a good agreement was observed for the center temperature and the mass loss of the brick. The slight difference is due to the assumptions made for the brick structure and the approaches in the modeling.

CONCLUSIONS

The results from this research which develops a model of simultaneous heat and mass transfer between the cavity and the porous source of humidity lead to the following conclusions:

- By this research, a model of simultaneous heat and mass transfer between the cavity and the porous source of humidity was developed implementing the relations between the vapor generation and diffusion. Thus, the phase change which FLUENT® is not able to solve, can be modeled by means of UDFs.
- "Interior" type boundary condition was chosen for the brick to be able to model the water vapor transport between the cavity and the brick.
- "Realizable k-ε" turbulence model was chosen among the other after comparing them for computational time, residuals and the consistency with the experimental results.
- The results of the computational studies were compared with the experimental results for the center temperature and mass loss of the brick and a good agreement was observed. By this model, simultaneous heat and mass transfer for different parameters in a cavity with a mass source can be investigated.

ACKNOWLEDGEMENTS

The authors would like to thank Arcelik R&D personnel and managers for their valuable contributions and financial support.

REFERENCES

[1] Chen, H. Q., Marks, B. P., & Murphy, R. Y., Modeling coupled heat and mass transfer for convection cooking of chicken patties, *Journal of Food Engineering*, Vol. 42, No.3, 1999, pp. 139-146.

[2] Thorvaldsson, K., & Janestad, H., A model for simultaneous heat, water and vapour diffusion, *Journal of Food Engineering*, Vol. 40, No.3, 1999, pp. 167-172.

[3] Lostie, M., Peczalski, R., Andrieu, J., and Laurent, M., Study of sponge cake batter baking process, Part I: Experimental data, *Journal of Food Engineering*, Vol. 51, No. 2, 2002, pp. 131-137.

[4] Shilton, N., Mallikarjunan, P., & Sheridan, P., Modeling of heat transfer and evaporative mass losses during the cooking of beef patties using far-infrared radiation, Journal of Food Engineering, Vol. 55, No. 3, 2002, pp. 217-222.

[5] Neale, A., Derome, D., Blocken, B.& Carmeliet, J., Coupled simulation of vapour flow between air and a porous material, *Proceedings of Thermal Performance of the Exterior Envelopes of Whole Buildings X Conference*, Clearwater Beach, FL, U.S.A, pp. 11-18, December 2007.

[6] Thorvaldsson, K., & Skjoldebrand, C., Water diffusion in bread during baking. *Food Science and Technology-Lebensmittel-Wissenschaft & Technologie*, Vol. 31, No. 7-8, 1998, pp. 658-663.

[7] Le Page, J. F., Chevarin, C., Kondjoyan, A., Daudin, J. D. and Mirade, P. S., Development of an approximate empirical-CFD model estimating coupled heat and water transfers of stacked food products placed in airflow, *Journal of Food Engineering*, Vol. 92, No. 2, 2009, pp. 208-216.

[8] BSI (2002). *EN 50304: Electric Ovens for Household Use, Methods for Measuring Energy Consumption*, UK: British Standards Institution.

[9] FLUENT, *FLUENT 6.2 user's guide*. Lebanon, New Hampshire, USA: Fluent Inc., 2005

[10] Kayihan A., Effect of ventilation system on heat and mass transfer inside a heated cavity having a moisture source (In Turkish), PhD Thesis, Istanbul Technical University, Istanbul, Turkey, 2011.

[11] ASHRAE handbook fundamentals (I–P ed., pp. 23.14). Atlanta, Georgia, USA, 2005.

[12] Onbasioglu, S.U., Kayihan, A. & Yilmaz, D., Modeling of Condensation and Evaporation with CFD (In Turkish), *The 10th HVAC& Sanitary Congress and Exhibition* , Izmir, Turkey, 2011.